8109/95

INTERPLANETARY DISCONTINUITIES AND ALFVÉN WAVES AT HIGH HELIOGRAPHIC LATITUDES: ULYSSES

Bruce T. Tsurutani, C. M. Ho, J, IS. Arballo, E. J. Smith, B. E. Goldstein, M. Neugebauer
Jet Propulsion Laboratory
California Institute of Technology
Pasadena, California 91109

A. Balogh
Imperial College of Science & Technology
The Blackett Laboratory
Prince Consort Road
London, England

and

W. C. Feldman
Los Alamos National Laboratory
Los Alamos, New Mexico 87545

ABSTRACT

This paper presents the results of the first statistical study of interplanetary directional discontinuities at high heliographic latitudes. We find that the rate of occurrence of interplanetary discontinuities (ROIDs) increases dramatically as Ulysses goes from the ecliptic plane to high (-80°) heliographic latitudes. The increase is about a factor of five as Ulysses moves from Jupiter at 5.4 AU to 2.5 AU over the south pole. There is a one-to-one correspondence between high ROID rates and when Ulysses is in a high speed stream. This is particularly dramatic just after Jovian encounter when there are. 25.5-day period corotating streams present. Thus, the increase with latitude is primarily due to Ulysses spending more and more percentage time within a high speed stream emanating from the solar coronal hole. High speed streams are characterized by the presence of nonlinear Alfvén waves with transverse fluctuations as large as $\Delta\vec{B}/|B|$ of 1 to 2. The normalized transverse wave power can be characterized by $P = 5 \times 10^{-4} f^{1.6}$ Hz^{-1}. The Alfvén waves are found to be propagating outward from the Sun, even at these large heliocentric distances. The waves typically have arc-like polarizations, and conserve field magnitude, to first order. Excluding stream-stream interaction regions, the normalized wave power spectra in different regions of the polar coronal hole streams, from the ecliptic plane to high heliographic latitudes, appear to be similar. Directional (rotational) discontinuities often form the edges of the phase-steepened Alfvén waves, thus offering a natural explanation of the ROID increase with increasing latitude. Discontinuities in the middle latitude regions are statistically more compressive than ones in the ecliptic plane. One possible explanation is that stream-stream interactions during the midlatitude excursion led to Alfvén wave coupling to compressive wave modes and eventual wave dissipation. This topic will be the subject of a further investigation.

INTROD[JCTION

One of the fundamental microstructure within the solar wind are directional discontinuities (DDs), sharp angular changes in the interplanetary magnetic field (Burlaga, 1969), These DDs are a mixture of both rotational (RD) and tangential (TD) discontinuities, as described by Landau and Lifschitz (1960) [see also Neugebauer et al. (1984)].

Several past works have focused on the radial gradients of their occu rence frequency (Burlaga, 197 1; Mariani et al., 1973; Behannon, 1978; Tsurutani and Smith, 1979, Lepping and Behannon, 1986). Although most past spacecraft trajectories have been confined primarily close to the ecliptic plane, potential latitudinal gradients have been derived (Mariani et al., 1973; Tsurutani and Smith, 1979). These latter results were based on data taken within only 10° to the ecliptic plane.

Complicating such studies of radial and latitudinal gradients are a possible dependence On coronal origin and dynamical evolution in interplanetary space (Neugebauer and Alexander, 199 1). It has been previously pointed out that the near- ecliptic variations in rate of occurrence are too large to be accounted for by statistical variations alone (Tsurutani and Smith, 1979). Orders of magnitude variation have been previously noted, Clearly, there must be other factors involved as well. Some of these have been identified and discussed in Neugebauer and Alexander (199 1) and Tsurutani et al, (1994; 1995a).

This paper explores the rate of occurrence of interplanetary discontinuities (ROIDs) as the Ulysses spacecraft goes from 1 AU to 5 AU in the ecliptic plane and then to high southern latitudes (-80°) at 2.5 AU. A strong positive latitudinal gradient will be demonstrated, We will demonstrate that this apparent gradient is due to the presence of high-speed, high-latitude stream structures. Solar wind plasma data will be used to demonstrate this dependence.

METHOD OF ANAl .YSIS

In this paper, interplanetary discontinuities are identified using two slightly different criteria. Tsurutani and Smith (1979), hereafter referred to as the. TS criteria, requires a field directional change of $\Delta\vec{B}/|B| \geq 0.5$ and $|\Delta B|$ greater than 26, where $\delta^2 = \sigma^2$, the variance on either side of the discontinuity. These criteria were applied to one minute averages, where the two one-minute vectors that are compared were separated by three minutes, This vector separation allows for discontinuities with “thicknesses” as large as 60s to be detected without bias. Thicker

discontinuities can be detected depending on their (tempora placement relative to the two vectors and the total angular change of the discontinuity.

We also use a slightly modified Lepping and Behannon (1986) criteria (hereafter referred to as the LB criteria). In this paper, wc require that the field directional change between vectors be at least 30", or $\theta = \cos^{-1}(\vec{B}_1 \cdot \vec{B}_2)/|B_1||B_2| \geq 30^\circ$. $\vec{B}_1$ ar id $\vec{B}_2$ arc the upstream and downstream vectors, respectively. There are several other features of the LB criteria that have been followed but are not repeated here, for brevity. This criteria was applied to one-minute averages, with $\vec{B}_1$ and $\vec{B}_2$ separated by two minutes. The primary difference in our current method and the original LB method is the duration of the data averages used (one minute versus 42s).

In Tsurutani et al. (1994) it was shown that the two criteria were quite similar. The TS criteria are slightly less stringent, so that they yield about a ~50% higher rate of discontinuities. The methods of computer selection of directional discontinuities were developed by TS and LB because statistical studies typically involve thousands of events. In this paper, we will identify over 35,000 discontinuities using both criteria.

Once directional discontinuities have been identified by computer selection, further analyses are done on higher time resolution data, For minimum variance analyses, field vectors within the discontinuity itself (sometimes as "thin" as 10s or less) need to be. examined. For this purpose, we use the highest time resolution available, 1 magnetic vector/s. Minimum variance analyses (Sonnerup and Cahill, 1967; Smith and Tsurutani, 1976) are pet-formed on these high resolution data to determine the direction of the normal.

The standard method of identifying the type of discontinuity, rotational or tangential, requires the determination of the magnetic field component along the normal direction (B_N) relative to the larger field magnitude on either side of the discontinuity (B],), and the jump in field magnitude ($\Delta|B|$) relative to B_{L}. Smith (1973, a, b) plotted each discontinuity as a point in phase space ($B_N/B_L, \Delta|B|/B_L$) on a scatter plot, We will follow the same procedure here. RDs are events with large B_N/B_L and small $\Delta|B|/B_L$, and TDs are events with large $\Delta|\vec{B}|/|B|$ and small B_N/B_L. Specific criteria will be discussed later,

Because there are often waves and other features present near the discontinuities, past experience has shown us that manual analysis is the best means to determine the most accurate values of B_L and AIB 1. We follow that method here. B_N is determined from the minimum variance analysis results. Because the determination of the phase space coordinate of each discontinuity requires

considerable effort, only several hundred discontinuities out of the tens of thousands of discontinuities have been examined in this manner during this study.

The temporal resolution of the Ulysses plasma data is not sufficient to aid in the detailed analysis of discontinuity types and features. Thus, we usc the plasma information only for the examination of solar wind flow type and phase relation to solar wind stream structures, etc. All detailed discontinuity analyses will be performed on the magnetic field alone.

RESULTS

ROID Radial and Latitudinal Gradients

The TS and LB discontinuity selection criteria have been performed on one minute averages of the magnetic field vectors for the Ulysses mission, from launch in October, 1990 to high heliographic latitudes during the first solar polar pass, September 1994. The rate of occurrence of interplanetary discontinuities (ROIDs) in the ecliptic plane from 1 to 5 AU, is shown in Figure 1. The vertical scale is the normalized number of discontinuities per day with 0.2 AU bins. The normalization takes any data gaps into account.

The TS and LB ROID values are shown as the solid plot and dashed plot, respectively. Both plots indicate a gradual decrease in rate of occurrence with increasing radial distance, They are fit by curves that fall off exponentially with increasing radial distance. The TS plot is best fit with a function of the form $e^{-(r-1)/5}$ and the LB plot is best fit with $e^{-(1-1)/4}$ where r is measured in AU. The ROID decrease with radial distance is presumably due both to an increase in discontinuity thickness, therefore falling outside of the selection criteria, and to dissipation of discontinuities.

Figure 2 gives TS and LB ROID plots and curve fits for the post-Jupiter encounter when Ulysses traveled to large negative heliographic latitudes. We show the ROID values from 0° to -80" latitude. Several features can be noted in the Figure. First we note the factor of -4 to 5 increase in ROID rate from -0° to -80". This dramatic increase is easily apparent in the two plots and two curves, and is a long term trend. The TS and LB ROID values increase more or less monotonically with time and latitude, based on 3 degree average values.

The gradual increase in the ROID values with latitude can be understood physically if one examines the detailed ROID dependence on stream structure. For this purpose, daily averages

are used, as displayed in Figure 3. From top to bottom are: the solar wind proton density, proton temperature, solar wind speed magnetic field magnitude, TS ROID rate, LB ROID rate, and the spacecraft location (radial distance from the Sun, and heliospheric latitude).

Several features can be noted in the Figure. Most important is that the ROID value depends strongly on the type of stream structure within which Ulysses is embedded. From the late part of 1992 (July) through April 1993, there are recur-ring, high speed streams at Ulysses (Bame et al., 1993; Phillips et al., 1994) associated with a coronal hole that is centered at the south pole of the Sun. This stream corotates with a -25.5 day period (Tsurutani et al., 1995b). The TS and LB ROID value increases and decreases in coincidence with the speed of the solar wind. Figure 3 shows this one-to-one correlation. When Ulysses is within the high speed stream, there are >80 discs day $^{-1}$ (TS criteria). When Ulysses is in a slow speed stream, there are less than 40 discs day $^{-1}$ ('I'S criteria). The above numbers were the extreme limits. A typical ratio of ROID value in a high speed stream to the value outside a stream is 4 or 5:1, After August 1993, the spacecraft became embedded in a high speed stream (through the end of this plot). The solar wind speed then remained generally high (-700 -800 km s-1) but decreases slightly with increasing latitude and decreasing radial distance. Correspondingly, the TS ROID values maintain a high value ranging between 80-100 discontinuities/day (see also Figure 2),

Alfvén Wave Properties

One of the fundamental discoveries of the Ulysses high latitude pass is the presence of large amplitude Alfvén waves in the solar wind (Tsurutani et al., 1994, 1995a; Smith et al., 1995a; Balogh et al., 1995a, Goldstein et al., 1995), as is illustrated in Figure 4. The data are presented in the Solar Heliospheric (SH) or RTN coordinate system. In this system $\hat{R}$ is directed radially away from the sun, $\hat{T}$ is defined by $(\hat{\Omega} \times \hat{R})/|\hat{\Omega} \times \hat{R}|$ where $\hat{\Omega}$ is the solar rotation axis, and $\hat{N}$ completes the right-hand system. The three components of the solar wind velocity and magnetic field are shown in this system. The radial component of the solar wind velocity (V_R) lies within a very narrow range of -735 to -820 km s^{-1}. The high frequency field fluctuations are large in all three components, but perhaps largest in B_T and B_N (here we ignore the larger slow -12 hour variations in V_R and concentrate on the high frequency variations). $\Delta\vec{B}/|B|$ is typically -1 to 2, indicating that these waves are highly nonlinear. Tsurutani et al., (1994) have shown that an intimate relationship exists between the fluctuations and discontinuities, a topic that we will examine again, later in this paper.

Figure 5 illustrates the results of a cross-correlation analyses between the SH components of $\vec{V}$ and $\vec{B}$ in a 24-hour interval of Figure 4. It is found that there is a strong correlation coefficient (c.c.) at zero lag (0.64, 0.86 and 0.85 c.c., respectively), indicating that these waves are indeed Alfvénic (see Belcher and Davis, 1971; Tsurutani et al., 1990). The sign of the correlation coefficient indicates that the waves are propagating outward from the sun.

Alfvén Waves and Discontinuities

In order to determine if the Alfvén waves and discontinuities arc different or similar at high latitudes from those in the ecliptic plane, we have selected six intervals of two days each to intercompare. These intervals were chosen such that they were Alfvén intervals within the trailing portions of high-speed streams. The intervals chosen are listed in Table 1. Also given are the two-day averages of the magnetic field magnitude, solar wind speed, proton density, and temperature and the Ulysses heliographic distance and latitude.

The intervals were selected to obtain a variety of radial distances from the sun and of heliographic latitudes. Two are near the ecliptic plane at different solar distances and four are at a variety of heliospheric latitudes.

Power spectra were calculated for each of the intervals. Because we wish to compare the field fluctuations at a variety of heliospheric distances from Sun where the magnetic field magnitudes are considerably different, we have normalized the power spectra by dividing by the average magnetic field magnitude squared. This latter quantity, wave power divided by $|B|^2$, is also a fundamental parameter used in the calculation of the effect of transverse waves in the (resonant) pitch-angle scattering of energetic particles (Kennel and Petschek, 1966).

Figure 6a gives the normalized wave power over a two-day period(wave power divided by $|B|^2$ when Ulysses was near the ecliptic and near -79° latitude. Panels 1) and 3) are one component of the transverse fluctuations at the two latitudes, and panels 2) and 4) are field magnitude spectra. Note that both the transverse and field magnitude power spectra at the two latitudes have frequency power law dependence of -1.6 to -1,7 (shown by the. curve fits). This is typical of all six intervals analyzed.

The intensities of the normalized wave power are slightly higher at the highest latitudes as quantified by the coefficients of the normalized power, At high latitudes, the coefficients are 2×10^{-4} and 2.4×10^{-5} for the transverse and B magnitude components. At low latitudes, the

coefficients are 1.0 x 10^{-4} and 1,1 x 10^{-5}, respectively. Thus, the normalized power at high latitudes are about a factor of -2 higher than that measured near the ecliptic plane.

The above normalized power spectra were calculated within a 10^{-1} to 10-4 Hz frequency interval. The frequency extent at the lower end is, of course, limited by the 2-day interval analyzed. Extension to lower frequencies requires longer time intervals. The result for an analysis of a ten day interval at the same two latitudes are shown as Figure 6b. Here, we again present normalized power spectra, 'but now over the frequency range between 10^{-5} and 10-2 Hz. The results are essentially the same for the high latitude interval [panels 3) and 4)], The ecliptic plane normalized wave power is however, considerably less. The reason for this is that the wave events in the ecliptic last only a few days and do not exist for a full 10 days. The spectra are therefore a mix of wave event plus generally more quiet solar wind conditions. The time average spectra are therefore generally less intense.

A histogram of the discontinuity "temporal" thicknesses using the TS discontinuities for days 154-155, 1994 (-67° latitude, 3.0 AU) is given in Figure 7. This is also one of the intervals in Table 1. High time-resolution magnetic field plots were used to generate these histograms. The 1/e value (65%) of the total angular change was used to define the thickness. Minimum variance analyses were performed on the data to determine the normal to the discontinuity. Using the "temporal thicknesses" and the minimum variance normal directions, we determine the spatial thicknesses of the discontinuities by equating the thickness to $V_{SW}\Delta t\cos\theta_{nv}$, where Vs_w is the solar wind velocity, At the "temporal thickness", and θ_{nv} the angle between the discontinuity normal and the solar wind velocity vector (the latter is assumed to be along $-\hat{R}$). The absolute thickness distribution in kilometers is shown in the bottom panel of Figure 7,

As previously mentioned, the TS method compares a one minute average vector with another which occurs three minutes later in time. Discontinuities with thicknesses 60s or less will thus be detected without bias. Discontinuities with thicknesses between 60 and 120s can also be detected without bias if their location in the time interval is well placed. Discontinuities which are thicker than 120s can also be detected if their vector change $\Delta\vec{B}/|B|$ is sufficiently large, > 0.5).

The study of the thickness distribution shown at the bottom of Figure 7 indicates that the increase in ROID value with increasing heliographic latitude cannot be explained by an increase in solar wind convection velocity alone (from ~400 km s-1 to ~750 km s-1). The distribution in panel 7a was taken during a high latitude interval where Vs_w was a constant -750 km s-1. If the

convection speed was lowered to -400 km s^{-1} (typical of the in-ecliptic speed), there would be fewer discontinuities detected. Only those with temporal thicknesses less than 32s (400 km s^{-1}/750 km s-1 x 60s) would be detected by our computer evaluation criteria. From Figure 7a, this would be 89 out of a total of 171 discontinuities, or a ratio of ~2.0. Of course, this is an overestimate, as the thicker discontinuities were not included in this calculation and the actual ratio would thus be less. However, the main point is that this cannot account for the factor of 4 to 5 increase in ROID rate in the interval where the corotating streams are present (see Figure 3), relative to when they are not. The increase in ROID values within the streams must be due to intrinsic properties of the high-speed stream medium itself.

Examples of the Alfvénic fluctuations and discontinuities are shown in Figure 8. The field is again plotted in SH coordinates. The vertical lines indicate the locations of the discontinuities identified by the TS criteria. The DDs are noted by sharp changes in the field components. Most discontinuities in this example are characterized by little or no change in field magnitude. The discontinuities are often found at the edges of the slowly changing field rotation, i.e., the Alfvén waves.

Figure 9 shows one of these waves plus discontinuity in higher time resolution. The total interval extends from 0728:10 to 0746:20 UT on day 154, 1994. The slowly rotating part of the wave occurs between 0728:10 to 0742:30 UT and the fast rotation associated with the discontinuity from 0742:30 to 0746:20 UT. The above times are indicated by the three vertical dashed lines.

The B_1 - B_2 minimum variance hodogram for the whole interval is displayed as the top panel of Figure 10. B_1 corresponds to the field in the maximum variance direction and B_2 to the intermediate variance direction. The polarization has an "arc-like" shape, (The arrows indicate the sense of vector rotation within the plane), The perturbation vector starts from the far left, rotates to the right, and then back to the left again, completing 360° in phase. There are other smaller waves present, causing some field fluctuations to be superposed on top of this general large amplitude rotation. When the slowly rotating part and the fast rotating part (the discontinuity) are separated, one gets the bottom-left and bottom-right hodograms, respectively. The same minimum variance coordinate system for the total wave plus discontinuity is used for both of the latter cases. The "Alfvén" wave part (left) contains approximately half of the phase rotation, rotating from the left to the right (-1800). The discontinuity is the other half, starting at the right and going to the left. Thus the slowly rotating Alfvén wave. plus discontinuity is an arc-

polarized phase-steepened Alfvén wave (Tsurutani et al., 1994), Cases such as these are present -30- 60% of the time in the high latitude Ulysses magnetic field data.

Although we note that the occurrence rate of discontinuities at high heliographic latitudes is much more constant than at lower, in-ecliptic locations, there is still some variability present at high latitudes. To address the question if this ROID variation is simply a statistical one, we construct a histogram of -6 months of data when Ulysses was at high heliographic latitudes at a nearly constant distance from the Sun (to remove any radial gradient effects). This is shown in Figure 11. The solid line indicates a symmetric curve fit to the data. Note that the half width at half maximum is 20 discontinuities/day. The peak of the distribution is -85 events/day. For a normal distribution, the standard deviation would be {85-= 9.2 and would correspond to the half-width. The actual distribution width is broader by a factor of more than twice that expected from statistical fluctuations alone.

Previous work has given us some hints as to what this additional variation might be due to. Tsurutani et al. (1994) noticed that the ROID can decrease to very low values (essentially zero) in a magnetic cloud/driver gas the reader should note that CMEs (near the Sun), interplanetary driver gases and magnetic clouds might not be identical; see Tsurutani et al., 1995b for discussion), Such low ROID value intervals can be noted for a few days within June, July, and August 1993 and February and April 1994 (see Figure 3). These have been confirmed to be driver gases by examining the magnetic fields in these intervals (this is believed by some of the authors to be the most reliable method to identify magnetic clouds, but it is still not 1009ZO effective). The exceptionally low ROID rates in the Jan-March histogram are due to the occurrence of these events. However, the general broadening of the distributions cannot be explained by this mechanism alone, as there are too few driver gas events in the data set. This problem will be addressed in subsequent works.

The discontinuity parameters B_N/B_L, $\Delta|B|/B_L$ have been previously used to identify discontinuity types (Smith, 1973). If B_N/B_L is large with a small value of $\Delta|\vec{B}|/B_L$, this identifies a rotational discontinuity (an ideal RI) has a (1.0,0) phase-space coordinate). An ideal tangential discontinuity has no normal component (B_N = O). Because a TD can separate plasmas with considerably different properties, $\Delta|B|$ can be different than zero. Thus following Smith (1973), we identify rotational discontinuities as those with $B_N/B_L \geq 0.4$ and $\Delta|B|/B_L$ c 0,2, Tangential discontinuities are identified as those with $\Delta|B|/B_L \geq 0.2$ and B_N/B_L <0,2, as shown in Figure 8, Discontinuities with $B_N/B_L \leq 0.4$ and $\Delta|B|/B_L \leq$ ().2 are indeterminate, and have properties of both RDs and TDs. The only clear way to determine the discontinuity type is to use

high time resolution plasma data (Neugebauer et al., 1984). Unfortunately, such data are not available for this study,

The results of a high time-resolution analysis of directional discontinuities for the interval Jan 20-21, 1991 are given in Figure 12. Ulysses was 1.8 AU from the Sun and near the ecliptic plane (-2.0"). Inspection shows that most of the discontinuities in the scatter plot have characteristics of rotational discontinuities. There is only one obvious tangential discontinuity.

Figure 13 illustrates the distribution for days 154-155, 1994 when Ulysses was at -67° heliographic latitude and -3.0 AU. Here again, there a lot of discontinuities that have rotational characteristics. However, a careful inspection shows that there are in addition a considerable number of events with tangential characteristics. There are also events with both large normal values and large field magnitude changes. The greater number of TDs and discontinuities with large B_N and $\Delta|B|$ is somewhat unexpected. At these latitudes, Ulysses is well above the heliospheric current sheet (a tangential discontinuity), which has been speculated to be fragmented at times (Crooker et al., 1993). Thus, these types of TDs should be absent in our present high-latitude set. The presence of Alfvén waves and their phase-steepened edges (RDs) at high latitudes would lead one to expect a large fractional number of RDs. Thus from this result, the TD/RD ratio would be expected to be lower at high latitudes rather than higher. Also, there are very few shocks at such high latitudes (Gosling et al., 1994; Smith et al., 1995b; Balogh et al., 1995b) and these discontinuities and their "I'D byproducts should be missing as well. The topic of tangential discontinuities and the discontinuities with large $|\Delta\vec{B}|/B_L$ and large B_N/B_L at high latitudes have been discussed briefly in Arballo et al., (1994) and Ho et al. (1995). This extensive subject will be postponed until future works.

The distribution of the normals to the TS discontinuities in the T-R and N-R planes for June 3-4, 1994 are given in Figure 14. Inspection shows that the discontinuity normals are nearly isotropic in directionality, There does not appear to be any preferred direction(s), except for possibly a slight k_R preference.

SUMMARY

A detailed analysis of Ulysses data reveals a decrease in the rate of occurrence of interplanetary discontinuities (ROIDs) with increasing heliocentric distance in the ecliptic plane and a dramatic increase in ROID rate with increasing heliocentric latitude. The heliographic latitude dependence was shown to be a function of the amount of time that Ulysses spent within a high-

speed stream which covers the south polar solar cap. The high-speed stream is characterized by nonlinear Alfvén waves with I $\Delta\vec{B}|/|B|$ -1-2. The waves are planar, arc-polarized and are often phase-steepened. The steepened edge of the wave is in the form of a rotational discontinuity. The waves are transverse oscillations, conserving field magnitude, to first order. The waves have a normalized power spectra I = 5 x $10^{-4} f^{-1.6}$ H Z-l. The normalized power spectral density frequency dependence is roughly constant over all heliographic latitudes and distances (within high-speed Alfvénic regions), and the intensity is a factor of two higher over the poles than at the equator (the latter might be, in part, a heliocentric distance aspect).

In the ecliptic plane, -80% of the discontinuities are found to be RDs. The other 20% are TDs or are mostly indeterminate. At high heliographic latitudes, wc find considerably more TDs and discontinuities with large field magnitude changes across the discontinuity interfaces. The breakdown is 58% RDs, 35% indeterminate, 6% TDs and 5% with large normals and |B| changes for the one interval shown. This is representative of the high latitude results (other intervals have been analyzed but are not shown). As previously mentioned, this new result will be the subject of a further work on TDs in the heliosphere.

The in-ecliptic ROID values decrease by a factor of 1.5- 2.() as Ulysses goes from 1 to 5 AU. This is somewhat less than that determined by the Tsurutani and Smith (1979) study using Pioneers 10 and 11 (a -2.'7 decrease). Several possible explanations come to mind. There could be temporal variations in the Ulysses data (these features were removed from the two spacecraft Pioneer 10 and 11 data sets). However, from this study and Tsurutani et al., (1994) we now know that the average rate of discontinuities is not a fixed value but depends both on how often magnetic clouds/driver gases are present in the data set and how much time the spacecraft remains within the Alfvénic region of high speed streams. These two factors depend upon the epoch of the solar cycle and the geometry of coronal holes. Thus, one implication of the Tsurutani et al. (1994) result and the results in this paper is that the ROID value may be very strongly solar cycle dependent.

Many of the pieces necessary to determine the dissipation rate of discontinuities are now in place: their normal directional distributions (isotropic), and the empirically determined thicknesses. This, plus in-situ solar wind velocity measurements, will allow a model of the discontinuity dissipation rate to be determined. This will be the next step in our efforts.

FINAL COMMENTS

This paper gives the first survey of discontinuities in the heliosphere covering both the ecliptic plane from 1 to 5 AU and high heliographic latitudes from 0° to -80". Together with information on the relative amplitude of Alfvén waves in coronal hole streams, this should be an important step towards understanding energetic particle transport over the poles. The wave power has been expressed in terms of $(\Delta\vec{B}/|\vec{B}|)^2$ such that both the theoretical pitch angle (Kennel and Petschek, 1966; Skilling, 1975) and cross-field diffusion rates (Tsurutani and Thorne, 1982) can be easily determined.

The finding that Alfvén waves are sometimes phase-steepened may have other important consequences. Phase steepening may be an important first-step process for wave "cascading", developing power at both higher and lower frequencies, and for eventual wave dissipation. The compressive components of discontinuities at the highest latitudes may indicate a coupling of Alfvén waves to compressive wave modes at these large distances.

Acknowledgments: Portions of this work were performed at the Jet Propulsion Laboratory, California Institute of Technology, Pasadena, under contract with the National Aeronautics and Space Administration. We wish to thank B, Robinson for his conscientious efforts in minimum variance analyses.

REFERENCES

Arballo, J. K., C. M, Ho, B. T. Tsurutani, J. S. Mok, E. J. Smith, B. E. Goldstein, M. Neugebauer, A. Balogh, D. J, Southwood, W. C. Feldman, Tangential discontinuities at high heliographic latitudes; Ulysses, EOS, 1994.

Balogh, A., E. J. Smith, B, T. Tsurutani, D, J. Southwood, R. J. Forsyth and T. S. Hornbury, The heliospheric magnetic field over the south polar region of the Sun, submitted to Science, 1995a,

Balogh, A., J. A, Gonzalez-Esparza, R. J. Forsyth, M. E. Burton, B. E. Goldstein, E, J. Smith and S. J. Bame, Interplanetary shock waves: Ulysses observations in and out of the ecliptic plane, Space Sci. Rev. 72, 171, 1995b.

Bame, S. J., B. E. Goldstein, J. T, Gosling, J. W. Harvey, D, J. McComas, M. Neugebauer and J. Phillips, Ulysses observations of a current high-speed solar wind stream and the heliomagnetic steamer belt, Geophys. Res. Lett, 20,2323, 1993.

Behannon, K. W., Heliocentric distance dependence of the interplanetary magnetic field, Rev. Geophys. Space Phvs., 16, 125, 1978.

Belcher, J. W. and L. Davis, Jr., Large amplitude Alfvén waves in the interplanetary medium, 2, J. Geophys Res., 76, 3534, 1971.

Burlaga, L. F., Directional discontinuities in the interplanetary magnetic field, Sol. Phys. 7, 54, 1969.

Burlaga, L, F., On the nature and origin of directional discontinuities, J. Geophys. Res., 76, 4360, 1971.

Crooker, N. U., G. L. Siscoe, S. Shodhan, D. F. Webb, J. T. Gosling, and E. J. Smith, J. Geophys. Res., 98, 9371, 1993.

Goldstein, B. E., M. Neugebauer and E. J. Smith, Alfvén waves, alpha particles and pickup ions in the solar wind, submitted to Geophys. Res. Lett., 1995.

Gosling, J. T., D. J. McComas, J, L. Phillips, L. Weiss, V. J, Pizzo, B. E. Goldstein, and R. J. Forsyth, A new class of forward-reverse shock pairs in the solar wind, Geophys. Res. Lett., 21, 2271, 1994.

Ho, C. M., B. T. Tsurutani, B. E. Goldstein, J. L. Phillips, and A. Balogh, Tangential discontinuities at high heliographic latitudes (-790), submitted to Geophys. Res. Lett., 1995.

Kennel, C. F., and H. F. Petschek, Limit on stably trapped particle fluxes, J. Geophys. Res., 71, 1, 1966.

Landau, L. D. and E. M. Lifschitz, Electrodynamics of Continuous Media, Pergammon, New York, 8, 224, 1960.

Lepping, R. P, and K. W. Behannon, Magnetic field directional discontinuities: Characteristics between 0.46 and 1.0 AU, J, Geophys. Res., 91,8725, 1986.

Mariani, F., B. Bavassano, U. Villante and N. F. Ness, Variations of the occurrence rate of discontinuities in the interplanetary magnetic field, J. Geophys. Res., 78, 8011, 1973.

Neugebauer, M., D. R. Clay, B. E, Goldstein, B. T. Tsurutani and R. D. Zwickl, A reexamination of rotational and tangential discontinuities in the solar wind, J. Geophys. Res., 89, 5395, 1984.

Neugebauer, M., C. J. Alexander, R. Schwenn and A. K. Richter, Tangential discontinuities in the Solar wind: Correlated field and velocity changes and the Kelvin-IIelmholtz instability, J. Geophys. Res., 91, 13694, 1986.

Neugebauer, M. and C. J. Alexander, Shuffling foot points and magnetohydromagnetic discontinuities in the solar wind, J. Geophys. Res., 46,9409, 1991.

Phillips, J. L., A. Balogh, S. J. Bame, B, E. Goldstein, J, T. Gosling, J, T. Hoeksema, D. J. McComas, M. Neugebauer, N. R. Sheely, Jr., and Y, M. Wang, Ulysses at 50° south: Constant immersion in the high-speed solar wind, Geophys. Res. I ett., 21,1105, 1994.

Skilling, J., Cosmic ray streaming, 1, Effect of Alfvén waves on particles, Mon. Nat. R. Astro. Soc. 172,557, 1975.

Smith, E. J., Identification of interplanetary tangential and rotational discontinuities, J. Geophys. Res., 78, 2054, 1973a.

Smith, E. J., Observed properties of interplanetary rotational discontinuities, J. Geophys. Res., 78, 2088, 1973b.

Smith, E. J, and B . T. Tsurutani, Magnetosheath lion roars, J. Geophys. Res., 81, 2261, 1976.

Smith, E. J., A. Balogh, R. P. Lepping. M. Neugebauer, J. Phillips and B. T. Tsurutani, Ulysses observations of latitude gradients in the heliospheric magnetic field, Ad. Space Res., 16, 165, 1995a.

Smith, E. J., M. Neugebauer, A. Balogh, S. J. Bame, R. P. Lepping, and B. T. Tsurutani, Ulysses observations of latitude gradients in the heliographic magnetic field: Radial component and variances, Space Sci. Rev. 72, 166, 1995b.

Sonnerup, B.U.O. and L. J. Cahill, Jr., Magnetopause Structure and attitude from Explorer 12 observations, J. Geophys. Res., 72, 171, 1967.

Tsurutani, B. T. and E. J. Smith, Inter'planetary discontinuities: Temporal variations and the radial gradient from 1 to 8.5 AU, J. Geophys. Res., 84, 2773, 1979.

Tsurutani, B. T., T. Gould, B. E, Goldstein, W. 1). Gonzalez, M, Suguira, Interplanetary Alfvén waves and auroral (substorm) activity: IMP-8, J. Geophys. Res., 95, 2241, 1990.

Tsurutani, B. T. and R. M. Thorne, Diffusion processes in the magnetopause boundary layer, Geophys. Res . Lett., 9 ,1247, 1982.

Tsurutani, B. T., C. M. Ho, E. J. Smith, M, Neugebauer, B. E. Goldstein, J. S. Mok, J. K. Arballo, A. Balogh, D. J. Southwood, and W. C. Feldman, The relationship between interplanetary discontinuities and Alfvén waves: Ulysses observations, Geophys. Res. Lett., 21, 2267, 1994.

Tsurutani, B. T., E. J, Smith, C. M. Ho, M. Neugebauer, B. E. Goldstein, J, S. Mok, A. Balogh, D. Southwood and W. C. Feldman, Interplanetary discontinuities and Alfvén waves, Space Sci. Rev., 72, 205, 1995a.

Tsurutani, B. T., C. M. Ho, J. K. Arballo, A. Balogh, Large amplitude IMF fluctuations in corotating interaction regions: Ulysses at midlatitudes, submitted to Geophys. Res. Lett. 1995b.

Table Captions

Table I. Six two-day Alfvénic intervals distributed in radial distance from the Sun and heliographic latitudes.

Figure Captions

Figure 1. The TS and LB in-ecliptic ROID values from 1 to 5 AU. Both plots are curve fit to exponential decay functions.

Figure 2. The TS and LB high-latitude ROID values. The values are covered over 3.0 degree intervals.

Figure 3. The daily average TS and LB ROID values as a function of solar-wind parameters. The ROID is 4-5 times higher when Ulysses is within a solar wind stream than when it is outside the stream.

Figure 4. Alfvénic fluctuations for July, 1994. The panels are the. R-T-N field and velocity components. Large $\Delta\vec{B}/|B| \sim 1\text{-}2$ fluctuations arc continuously present in the data.

Figure 5. The $B_R - V_R$, $B_T - V_T$, $B_N - V_N$ cross-correlations for 00-24 UT, day 165, 1994. All three correlations have peak positive values at zero lag, indicating, that the fluctuations are Alfvénic and are propagating outward from the Sun.

Figure 6. Normalized magnetic field power spectra for intervals at -2", 1.8 AU and -79", 2.4 AU. Panel a) is for two day intervals and covers 10^{-4} to 1 0^{-1} } Iz. Panel b) is for ten day intervals and the spectra covers 10-5 to 10^{-2} Hz.

Figure 7. Discontinuity thicknesses for events on days 154-155, 1994, The top panel a) is the I/e "temporal" thicknesses. Panel b) give the true spatial thicknesses where the normal direction and convection speed have been taken into account.

Figure 8. Vertical lines indicate the TS discontinuities for day 154, 1994.

Figure 9. An example of an Alfvén wave with a phase-steepened edge (RD). From left-to-right, dashed vertical lines give the start of the Alfvén wave, the start of the RD and the end of the RD.

Figure 10. Minimum variance hodograms of the phase-steepened rotation of the Alfvén wave plus RD (top), the slow rotation (bottom left) and the RD (bottom right). The slow rotation portion of the wave comprises a -160° phase rotation and the RI) another -200° phase rotation. The Alfvén wave is phase-steepened with an arc-polarization.

Figure 11. The ROID value distribution over 6 month interval (Jan-June 1994). The distribution is broader than one could expect from statistical fluctuations.

Figure 12. Discontinuity phase space (B_N/B_L, $\Delta|B|/B_L$) distributions for days 20-21, 1991. Most of the discontinuities are RDs.

Figure 13. Same as Figure 12, but for! days 154-155, 1994 at --67° latitude. There are now many more TDs and discontinuities with large $\Delta|B|/B_L$.

Figure 14. The normals to the discontinuities of day 154-155, 1994 in the RTN coordinate system.

ULYSSES Observations

Year	Day	B_{AVG} (nT)	V_{SW} (km/see)	n_p	Tp ("K X 10^4)	Radial Distance from Sun (AU)	Helio-spheric Latitude
91	020/021	1.69	384	().60	4.3	1.81	-1.9°
91	123/124	0.32	549	0.95	2.86	2.91	-4.4°
92	286/287	0.47	747	0.I()	4.6	5.21	-18.5"
93	183/184	1.04	760	0.22	4.2	4:5-7-	-33.8"
94	154/155	0.90	758	0.28	9.2	2.98	-66.6"
94	238/239	1.26	778	().4 1	11.2	2.42	-79.2"

Table 1

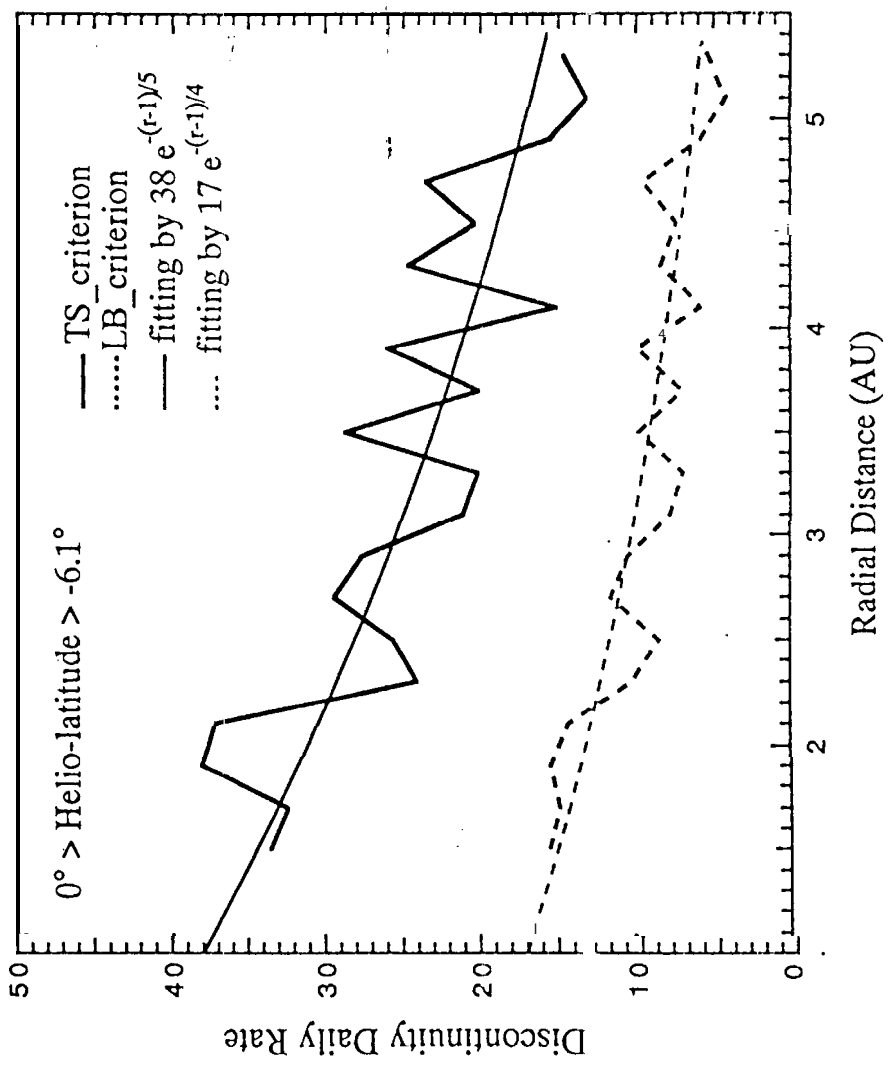
0° > Helio-latitude > -6.1°
TS_criterion
LB_criterion
fitting by 38 e^-(r-1)/5
fitting by 17 e^-(r-1)/4
Discontinuity Daily Rate
Radial Distance (AU)
0
10
20
30
40
50
2
3
4
5

FIG. 1

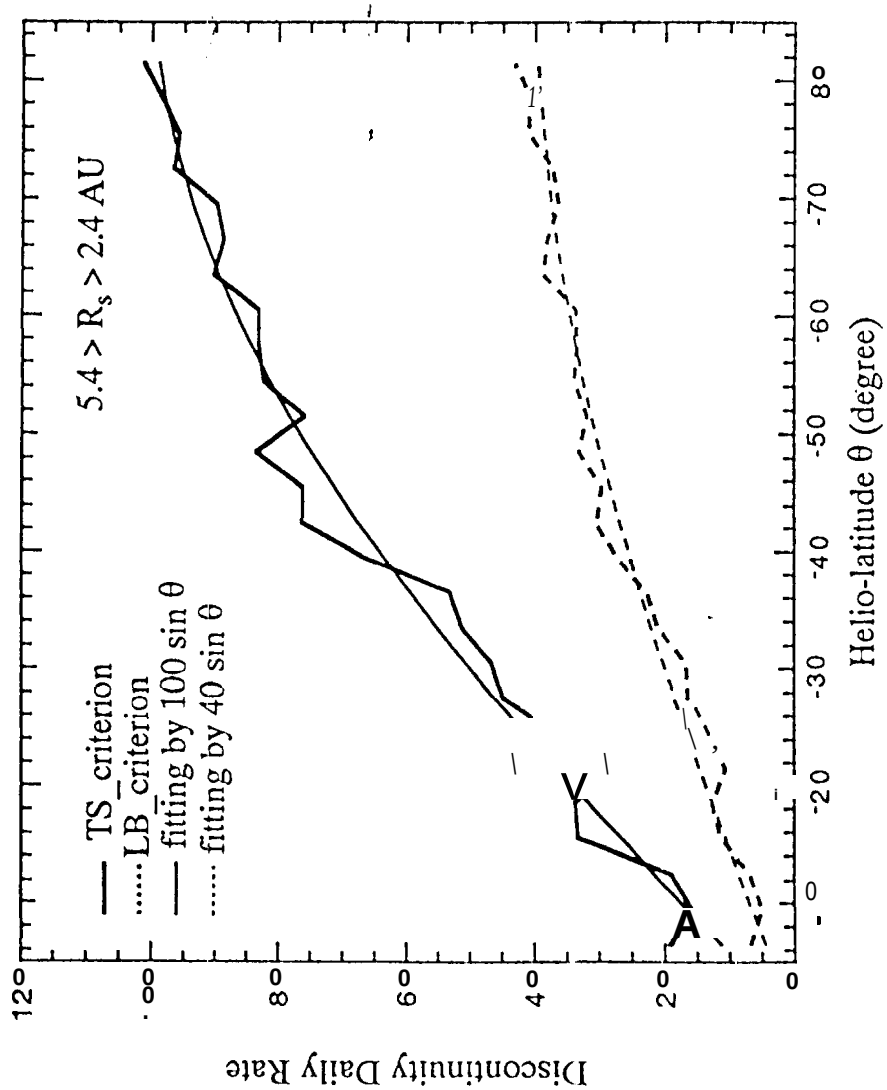
5.4 > R$_s$ > 2.4 AU
TS_criterion
LB_criterion
fitting by 100 sin θ
fitting by 40 sin θ
A
V
Discontinuity Daily Rate
Helio-latitude θ (degree)
120
100
80
60
40
20
0
-0
-20
-30
-40
-50
-60
-70
80

Fig. 2

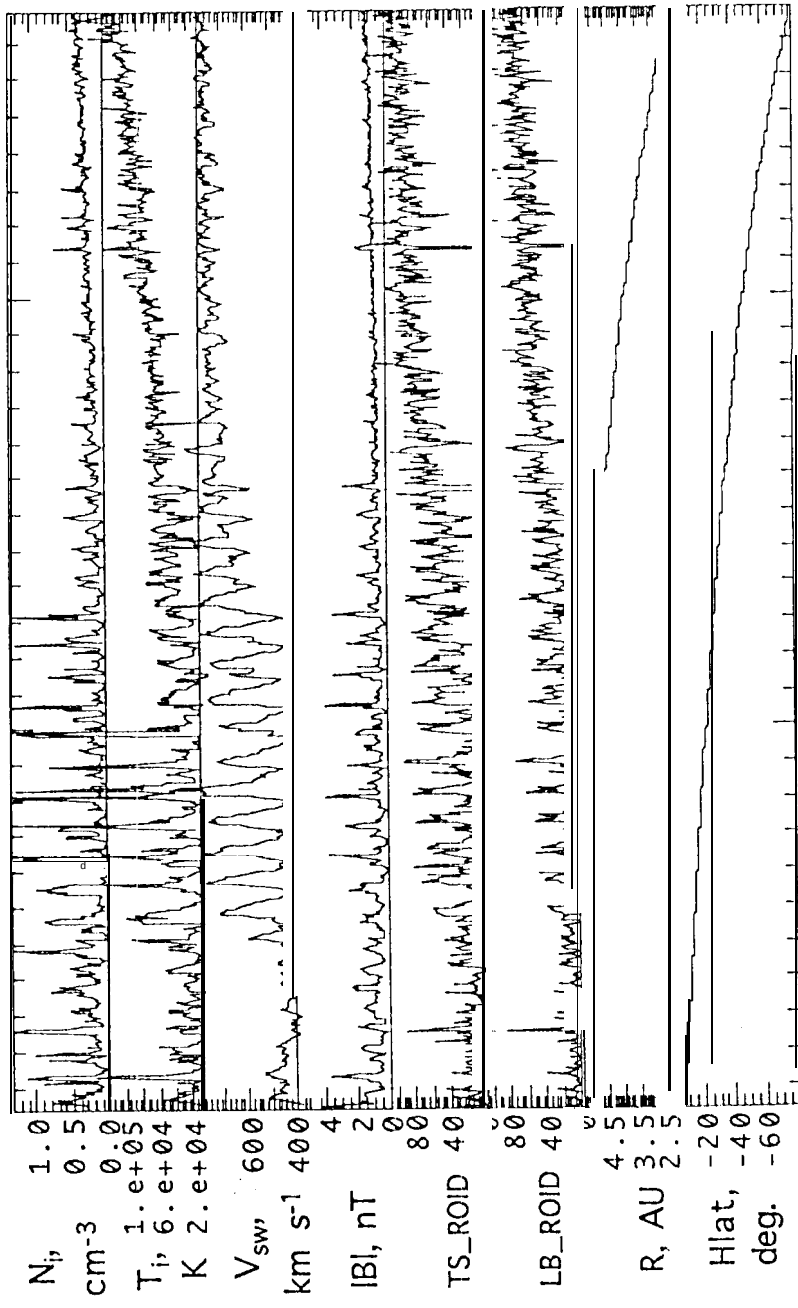
N_i, cm^{-3}
1.0
0.5
0.0
T_i, K
1.e+05
6.e+04
2.e+04
V_{sw}, km s^{-1}
600
400
|B|, nT
4
2
0
TS_ROID
80
40
LB_ROID
80
40
R, AU
4.5
3.5
2.5
Hlat, deg.
-20
-40
-60
92MAR
93JAN
94JAN
TIME (TIC=MONTH)

Fig. 3

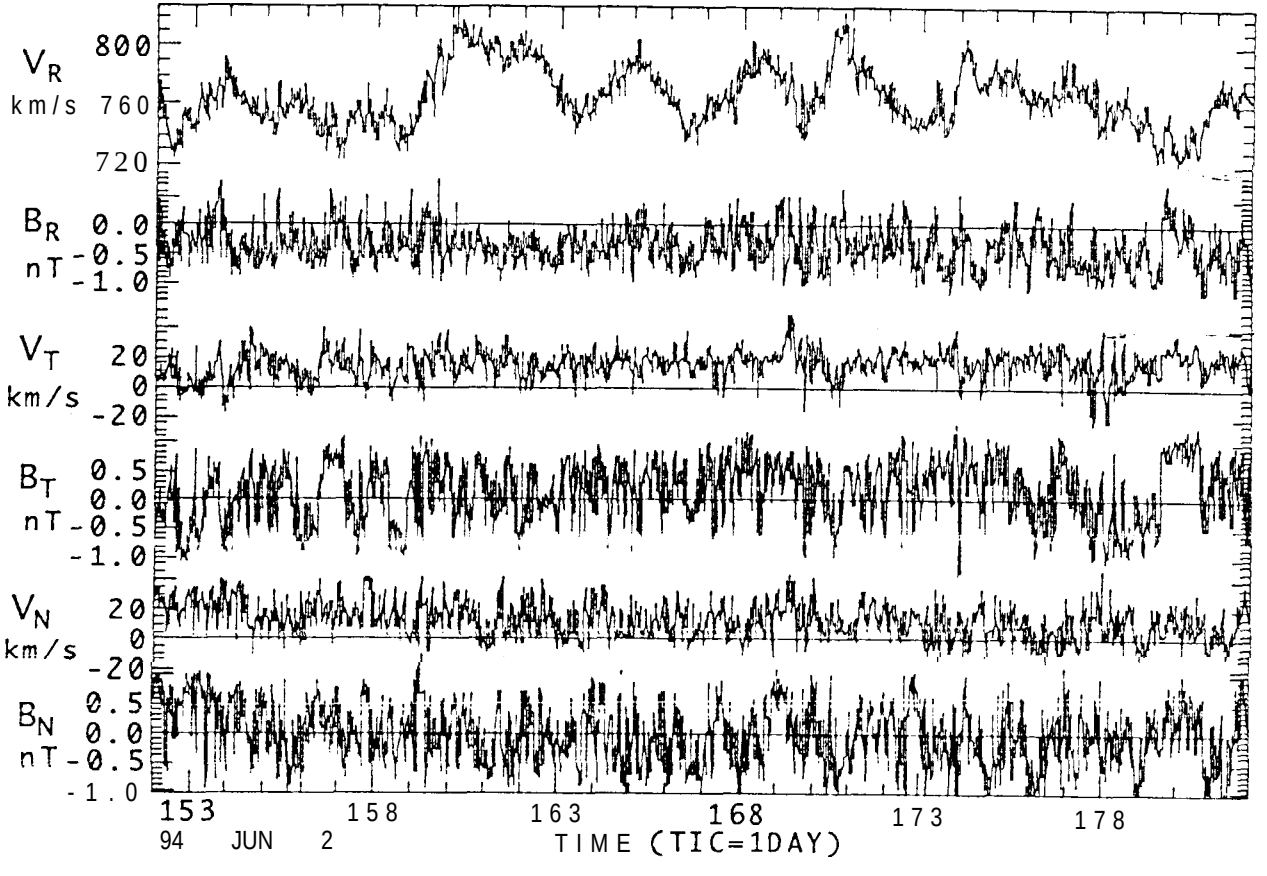
V_R
km/s 800
760
720
B_R 0.0
nT -0.5
-1.0
V_T 20
km/s 0
-20
B_T 0.5
nT 0.0
-0.5
-1.0
V_N 20
km/s 0
-20
B_N 0.5
nT 0.0
-0.5
-1.0
153
158
163
168
173
178
94 JUN 2
TIME (TIC=1DAY)

Fig 4

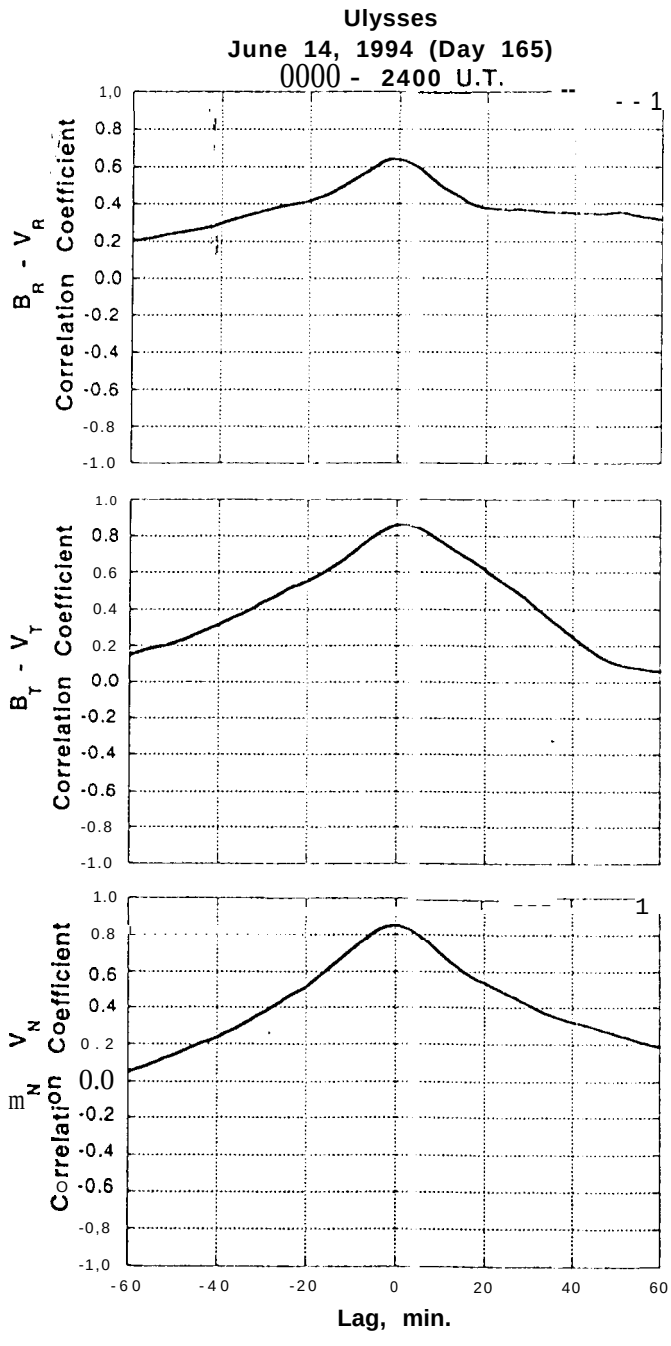
Ulysses
June 14, 1994 (Day 165)
0000 - 2400 U.T.
B_R - V_R Correlation Coefficient
B_T - V_T Correlation Coefficient
V_N m_N Correlation Coefficient
1.0
0.8
0.6
0.4
0.2
0.0
-0.2
-0.4
-0.6
-0.8
-1.0
-60
-40
-20
0
20
40
60
Lag, min.

Fig. 5

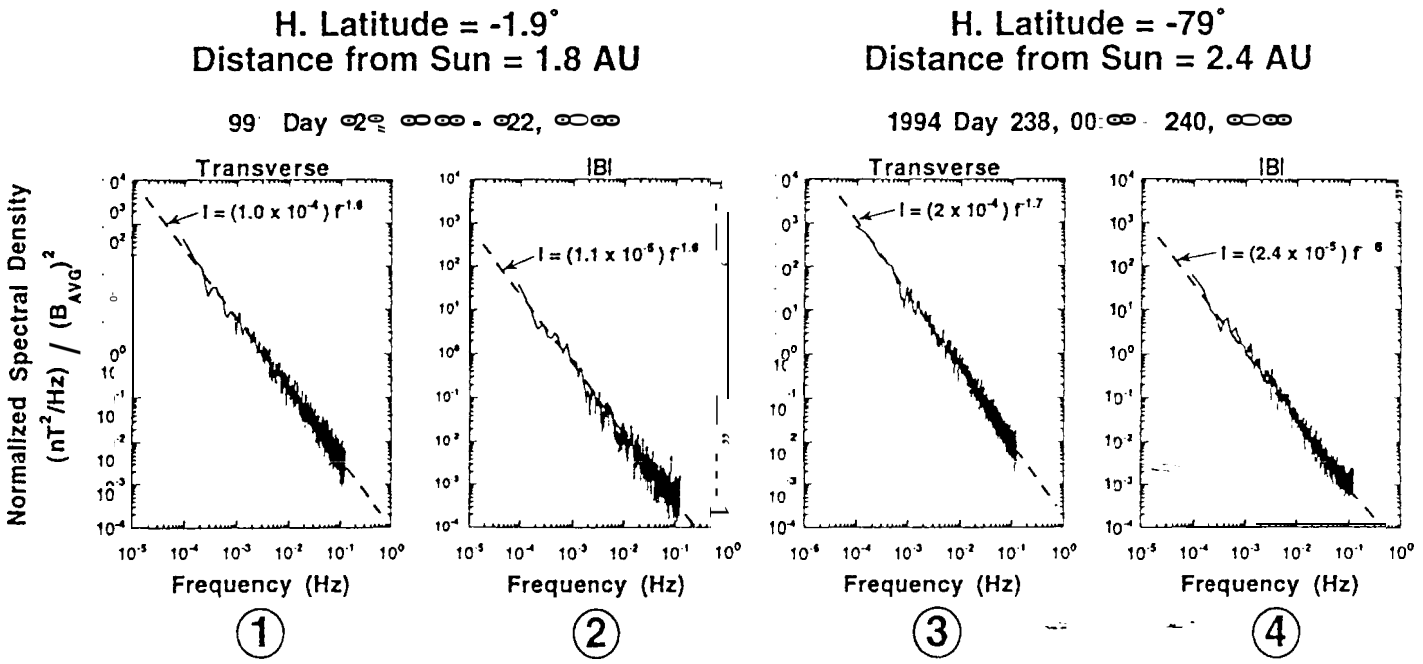

A) 2-day intervals

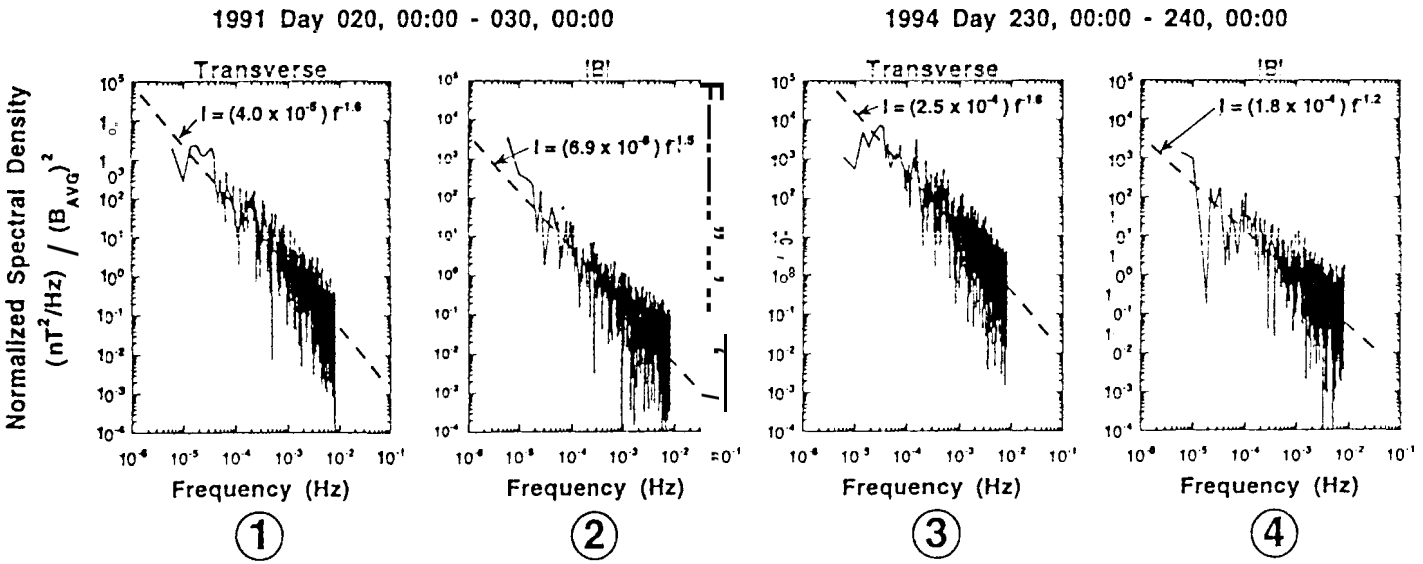

B) 10-day intervals

Fig. 6

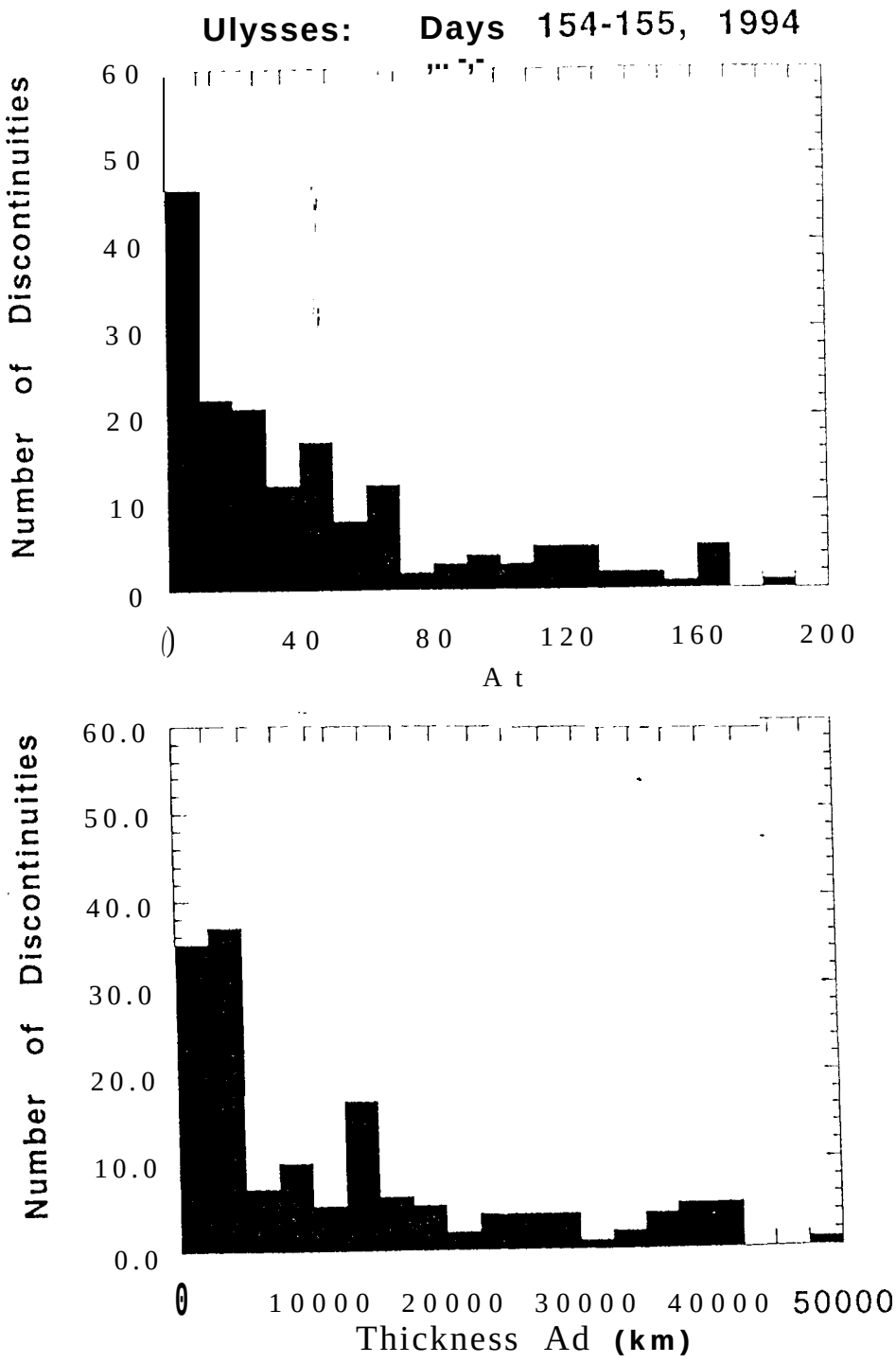
Ulysses: Days 154-155, 1994
Number of Discontinuities
60
50
40
30
20
10
0
0
40
80
120
160
200
At
Number of Discontinuities
60.0
50.0
40.0
30.0
20.0
10.0
0.0
0
10000
20000
30000
40000
50000
Thickness Ad (km)

Fig. 7

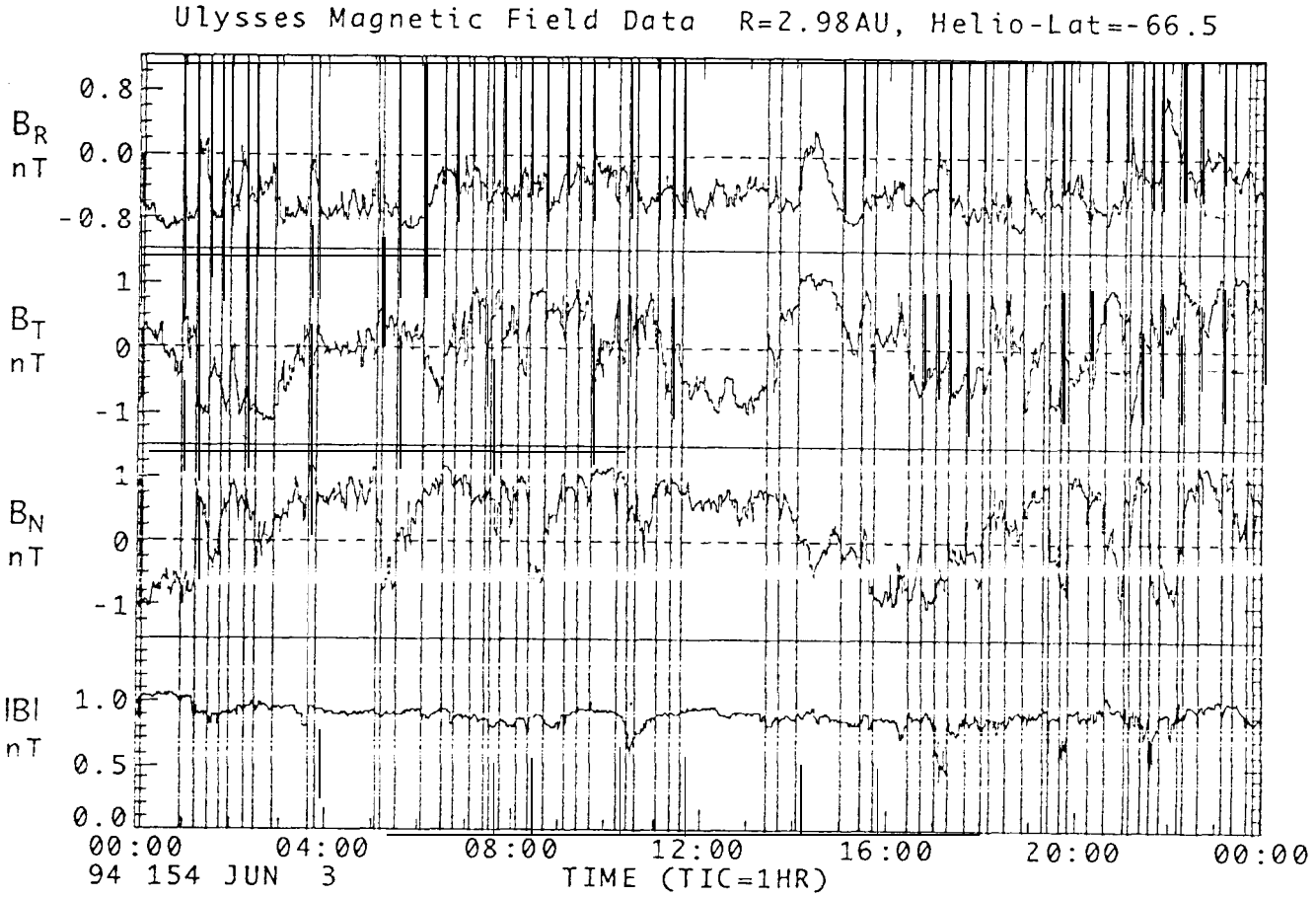
Ulysses Magnetic Field Data R=2.98AU, Helio-Lat=-66.5
B_R nT
0.8
0.0
-0.8
B_T nT
1
0
-1
B_N nT
1
0
-1
|B| nT
1.0
0.5
0.0
00:00
04:00
08:00
12:00
16:00
20:00
00:00
94 154 JUN 3
TIME (TIC=1HR)

F.J.8

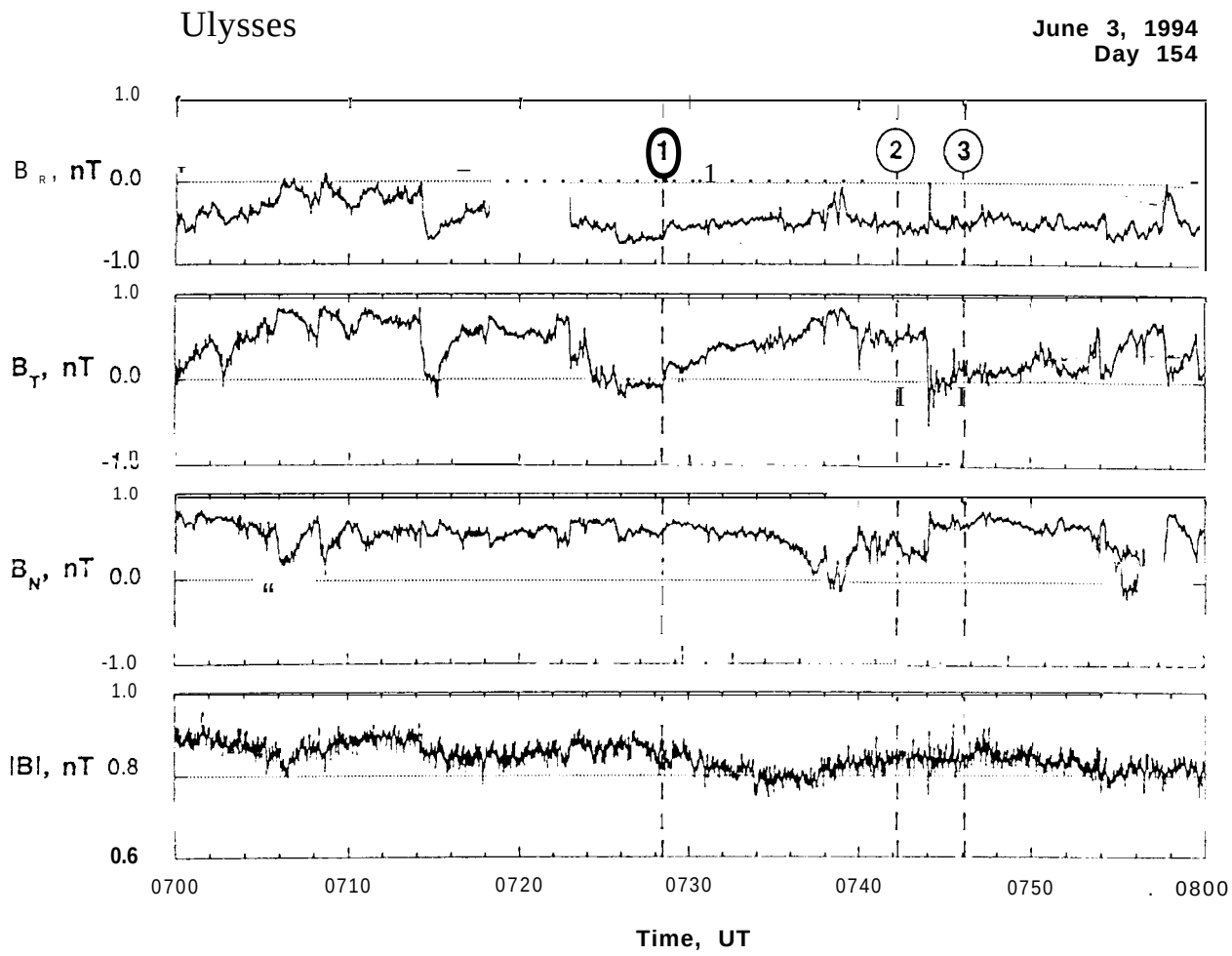
Ulysses
June 3, 1994
Day 154
1.0
B R, nT 0.0
-1.0
1
2
3
1.0
B T, nT 0.0
-1.0
1.0
B N, nT 0.0
-1.0
1.0
|B|, nT 0.8
0.6
0700
0710
0720
0730
0740
0750
0800
Time, UT

ULYSSES

June 3, 1994
Day 154

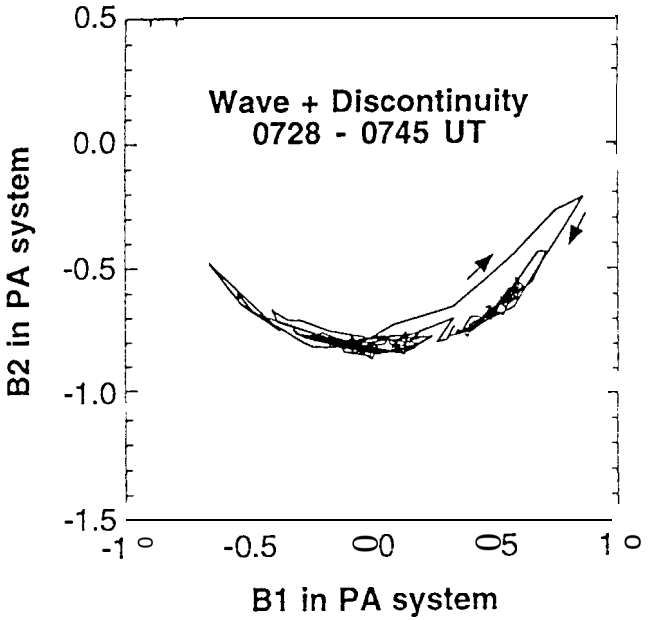

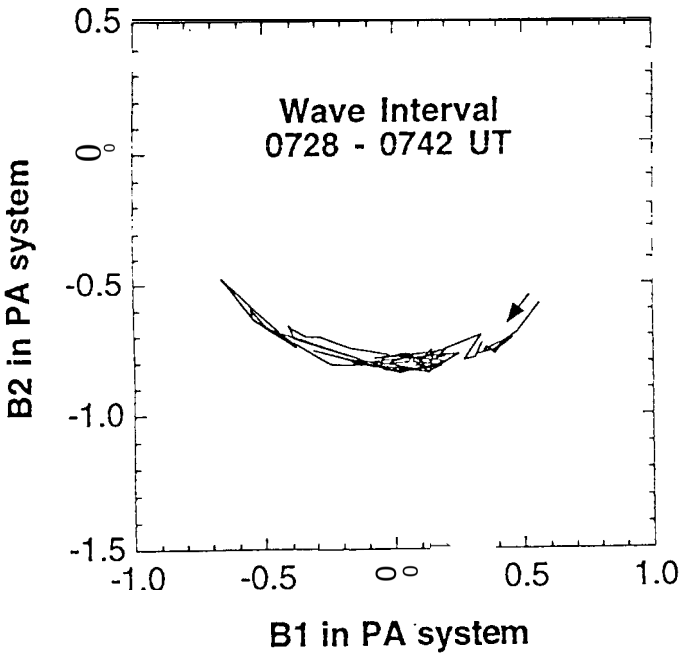

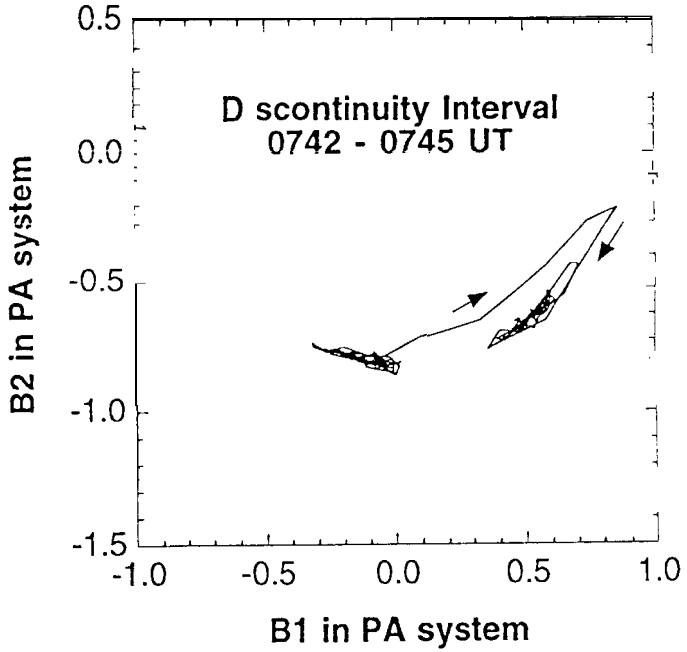

Fig 10

Tsurutani-Smith Criteria

Distribution of
Rate of Occurrence of Interplanetary Discontinuities (ROID)
at High Heliographic Latitude Regions
(January 1 - June 30, 1994)

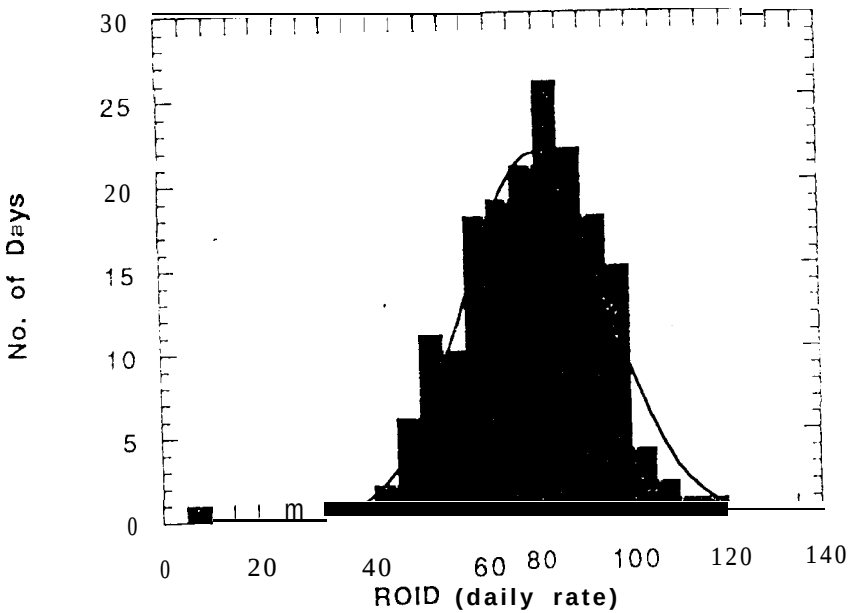

ULYSSES
1991 Days 020-021
a = 1.81 AU
x Lat = -1.9°
|ΔB|/B_L
m' / B_1
0
0.2
0.4
0.6
0.8
1.0

Fig. 12

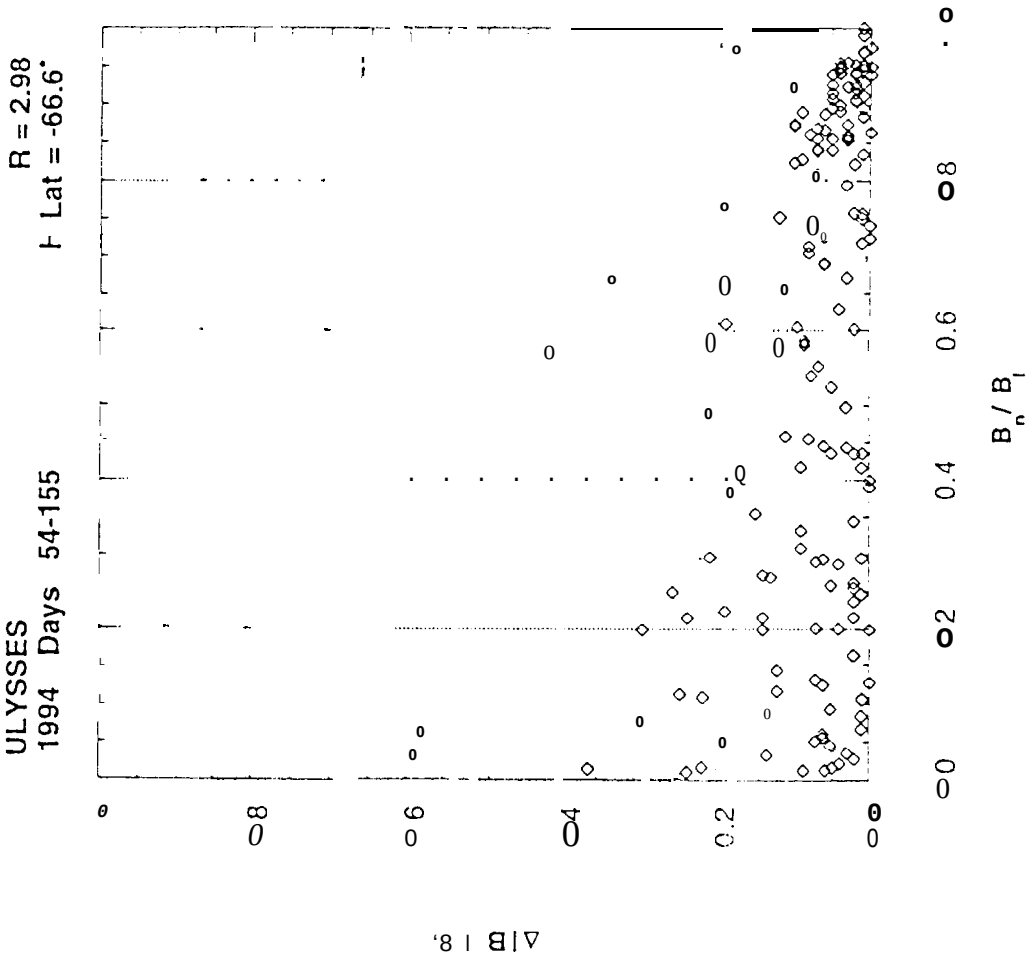

Fig. 13

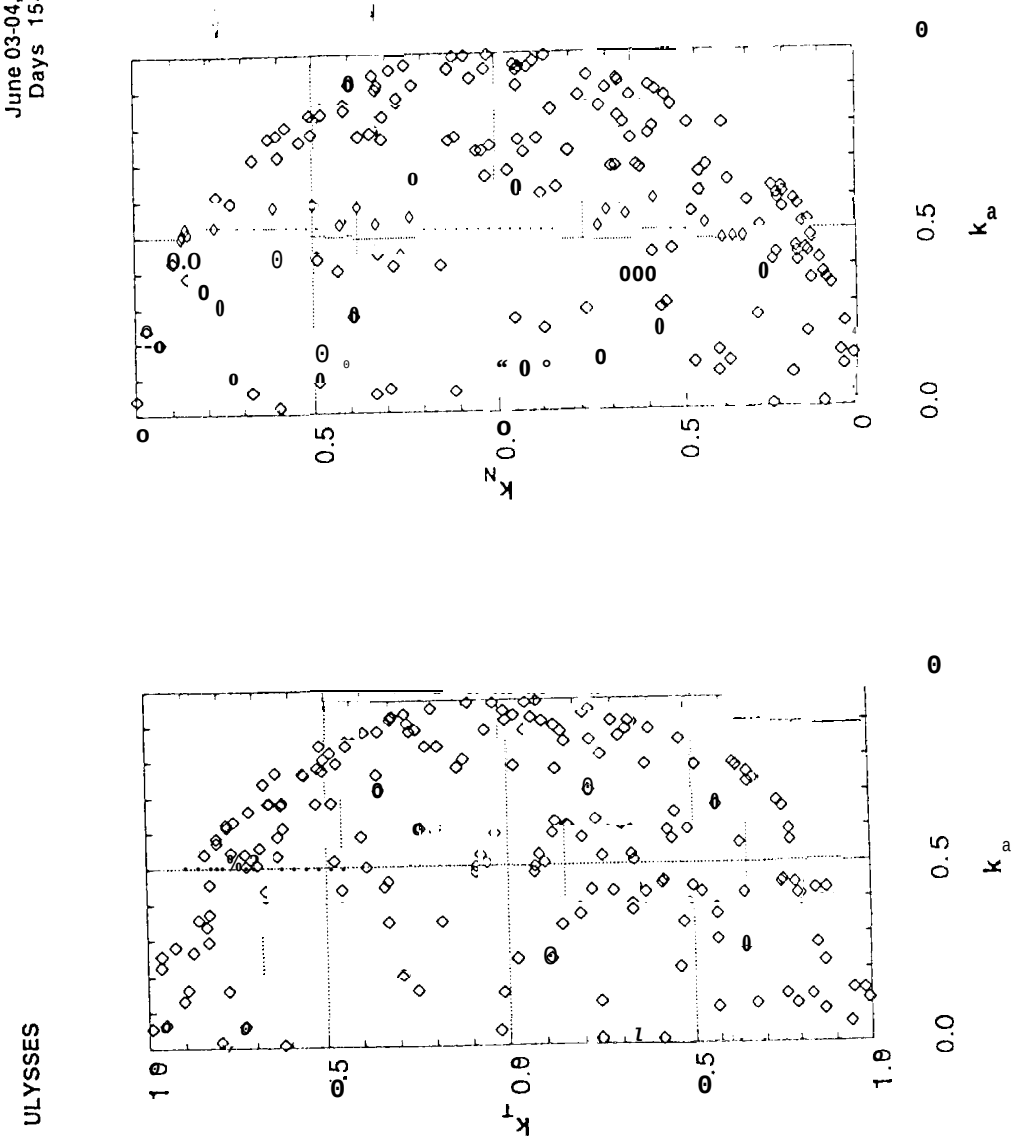

Fig. 14